ENGINEERING MICROWAVE PROPERTIES OF MICROWIRES

S. A. Baranov [1, 2]

[1]*Institute of Applied Physics, Academy of Sciences of Moldova, Academiei str. 5, Chisinau, MD-2028 Republic of Moldova*

[2]*Département de Génie Physique, École Polytechnique de Montréal, C.P. 6079, succ. Centre-ville, Montréal H3C 3A7, (Québec) Canada*

(Received December 04, 2014)

Abstract

A correlation between the frequency of natural ferromagnetic resonance (NFMR) (1−12 GHz) determined from the dispersion of permeability and alloy composition (or magnetostriction between 1 and 40 ppm) of glass-coated microwires has been systematically confirmed. Absorption of composite (microwire pieces embedded in a polymer matrix) screens has been experimentally investigated. Parallel theoretical studies suggest that a significant fraction of the absorption can be ascribed to a geometrical resonant effect, while a concentration effect is expected for the thinnest microwires.

Keywords: Amorphous magnetic microwires; Ferromagnetic resonance; Natural ferromagnetic resonance, high frequency properties

1. Introduction

Microwave engineering is of great importance in a wide spectrum of applications most of which are related to wireless telecommunications systems, such as telephone, broadcast satellite television, or satellite global positioning. Radar systems are also very useful for detecting mobile targets in air, sea, or ground, for air-traffic control or missile tracking radars, and for a wide variety of remote sensing systems. In addition, resonance phenomena appearing at microwave frequencies offer an opportunity for novel applications in heating systems, medical diagnosis and treatment or just new effects in basic science. In all these cases, the involved phenomena are characterized by millimeter electromagnetic waves with frequencies in a range of 300 MHz to 300 GHz.

The search for materials exhibiting outstanding properties in this frequency range is thus relevant in the development of the mentioned applications. Here, we focus on a particular family of materials, i.e., glass-coated amorphous magnetic microwires, exhibiting an exciting microwave behavior with enormous technological applications as elements for absorption of electromagnetic radiation.

Glass-coated magnetic microwires are characterized by a nucleus of a magnetic alloy, a structurally amorphous and metallic conductor, with a diameter between 2 and 20 μm, covered by a Pyrex-like coating with a thickness of 2−10 μm. They are prepared by quenching and drawing rapid solidification method, following the early Taylor technique later modified by Ulitovsky [1−4]. The coating, in addition to insulating the metallic nucleus from corrosion and electrical viewpoints, induces strong mechanical stresses in the nucleus, which, coupled with its magnetostriction, determine strong magnetoelastic anisotropy, in the origin of a unique magnetic behavior. Particularly, magnetic bistability characterized by a square low-field loop with a single giant Barkhausen jump is observed in magnetostrictive Fe-rich microwires [4, 5]. Alternatively, non-magnetostrictive Co-base microwires exhibit giant magnetoimpedance (GMI) effect, which originates in the electromagnetic classical skin-effect, observed in the radio frequency range [6−8]. GMI has been also correlated to ferromagnetic resonance phenomena appearing typically in the microwave frequency range [8]. In addition, glass-coated microwires also show interesting electromagnetic absorption properties as shown through different techniques like wave-guide experiments, through the scattering and the transmission coefficients, and in general the ferromagnetic-resonance (FMR)and antiferromagnetic-resonance (AFMR) behavior. Of particular interest is the natural ferromagnetic resonance (NFMR) observed as a consequence of a strong intrinsic magnetoelastic anisotropy.

The technological use of high and ultra-high frequencies in engineering has led to the need of creating electromagnetic protective screens. Amorphous microwires can be thus employed as radio-absorption elements when embedded in suitable matrices. Here, we introduce an analysis of the opportunity of application of these materials in composite protective screens.

2. Production and properties

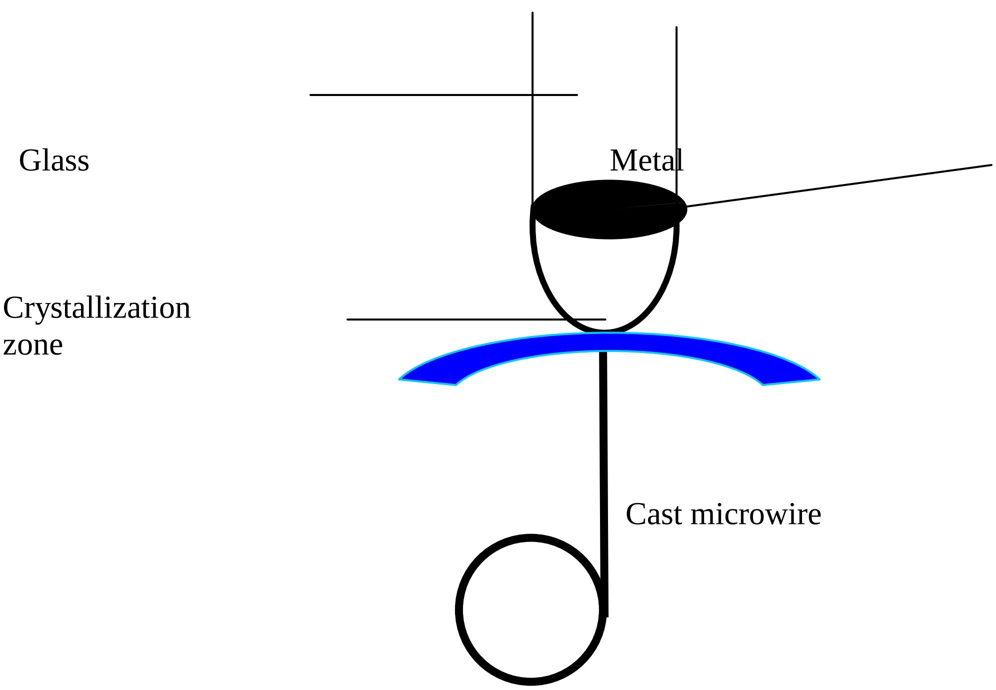

Fig. 1. Taylor−Ulitovsky method for fabrication of microwires.

Cast glass-coated amorphous magnetic microwires are produced by the Taylor−Ulitovsky method (see [1–4] and Fig. 1). The alloy is heated in an inductor up to the melting point. The portion of the glass tube adjacent to the melting metal softens and envelopes the metal droplet. Under suitable conditions, the molten metal fills the glass capillary and a microwire is thus formed with the metal core completely covered by a glass shell.

The microstructure of a microwire depends mainly on the cooling rate, which can be controlled when the metal-filled capillary enters a stream of cooling liquid in its way to the receiving coil. Critical quenching rates (10^5–10^7 K/s) for fabrication of amorphous materials can be obtained.

The glass coating of the cast amorphous magnetic microwires, in addition to protecting the metallic nucleus from corrosion and providing electrical insulation, induces large mechanical stresses in the nucleus. Coupled with its magnetostriction, these factors determine its magnetoelastic anisotropy, at the origin of a unique magnetic behavior. The residual stresses are the result of differences in the coefficients of thermal expansion of the metal and the glass. A simple theory for the distribution of residual stresses was presented in [2,3]. In cylindrical coordinates, the residual tension is characterized by axial, radial, and tangential components which are independent of the radial coordinate. The value of these stresses depends on the ratio of radius *r* of the metallic nucleus to total microwire radius *R*:

$$x = \left(\frac{R}{r}\right)^2 - 1,$$

$$\sigma_r = \sigma_\phi = P = \sigma_0 \frac{kx}{\left(\frac{k}{3}+1\right)x + \frac{4}{3}},$$

$$\sigma_z = P\frac{(k+1)x+2}{kx+1}, \tag{1}$$

where $\sigma_0 = \varepsilon E_1$; ε is the difference between the thermal expansion of the metallic core and that of the glassy cover with expansion coefficients α_1 and α_2: ($\varepsilon = (\alpha_1 - \alpha_2)(T^* - T)$); E_1 is the Young's modulus of the metal core, T^* is the solidification temperature of the composite in the metal/glass contact region ($T^* \sim$ 800–1000 K), T is the room temperature ($\varepsilon E_1 \sim 2GPa$ is the maximum stress in the metallic core).

Technological parameter k is the ratio of Young's moduli of the glass and the metal ($k = E_2/E_1 \sim$ 0.3–0.6). Numerical calculation indicates that, for small values of x, the dependence $\sigma_z(x)$ is almost linear and reaches saturation (up to 1GPa) at about x = 10:

$$\sigma_z \sim (2 \div 3) P > \sigma_r,$$

$$(P \to 0{,}5\sigma_0 \sim 1\ GPa)$$

The general theory of residual tension is presented in [5] where other calculations of residual tension are criticized. Here, we further analyze the case where the depth of the skin layer is less than nuclear radius *r*. In this case, Eq. (1) provides a good description of experiment (see below, Eqs. (11)−(13) and Figs. 2−4).

For materials with positive magnetostriction, the orientation of the microwire magnetization is parallel to the maximal component of the stress tensor, which is directed along the axis of the wire (see [1−3]). Therefore, cast Fe-based microwires with positive magnetostriction constant show a rectangular hysteresis loop with a single large Barkhausen jump between two stable magnetization states and exhibit the phenomenon of NFMR (see [1−3]).

The FMR method is often used for the investigation of amorphous magnetic materials (ribbons, wires, thin films). Both macroscopic and microscopic heterogeneity of amorphous materials can be investigated by FMR. Residual stress is an important parameter for amorphous materials which can be studied by FMR (see [1−3]).

FMR is also used for diagnostics of the uniformity of amorphous materials. Extrinsic broadening of FMR lines due to fluctuations of the anisotropy, magnetization, and exchange-interaction constant in amorphous materials has also been investigated. Microwave experiments are very useful for investigation of spin-wave effects. In particular, microwave generation and amplification are of great interest. Investigation of structural relaxation of amorphous materials during heat treatment using FMR is also important. Differential FMR curves combined with hysteresis curves can give important information in this case.

In the present work, cast glass-coated amorphous microwires with metallic cores and diameters of 0.5−25 μm were considered. The amorphous structure of the core was investigated by X-ray methods. The thickness of the glass casing varied between 1 and 20 μm. Using microscopy, samples with the most ideal form and with lengths of about 3−5 mm were selected for investigation. Microwires based on iron, cobalt, and nickel (doped with manganese), with additives of boron, silicon, and carbon were studied. Microwires made of different materials have diverse magnetostriction. We studied microwires from the same spool whose glass casing was removed by etching in hydrofluoric acid.

In almost all cases, standard FMR spectrometers of 2−32 GHz were used. The magnetic field was measured using a Hall sensor (with an accuracy within 0.1%). In addition, magnetometer measurements determined the magnetization needed for calculation.

The basic measurements were made in a longitudinal field configuration (the external magnetic field was directed along the microwire axis). In this case, a signal of a correct form was obtained from good samples. This gives the possibility of measuring resonant-curve width.

For thick cores, skin effect must be taken into account. In this case, the resonant frequency was described by the Kittel formula for a plane (with longitudinal magnetization). The *g* factor was estimated at two resonant frequencies as ~ 2.08 ÷ 2.1 on average. Our results are in good agreement with literature data on the *g* factor for amorphous materials (see[1−4, 6−8]). In a transverse field (when the external field is perpendicular to the microwire axis), the signal was weak or not observed in samples with negative magnetostriction. It is obvious that the presence of this signal is associated with non-uniformity of the high-frequency demagnetizing factor.

A microwire was considered to be a ferromagnetic cylinder with small radius *r*. To characterize it, we introduce following parameters.

1. The depth of the skin layer is:

$$\delta \sim [\omega(\mu\mu_0)_e \Sigma]^{-1/2} \sim \delta_0(\mu)_e^{-1/2}, \tag{2}$$

$(\mu\mu_0)_e$ is the effective magnetic permeability, and Σ is the electric conductivity of the microwire. In the case of our magnetic microwires, with the relative permeability |μ eht fo ecnanoser raen | order 10^2, (ω ~8–10GHz) δ changes from1 to 3μm.

2. The size of the domain wall (according to Landau−Lifshits theory) is

$$\Delta_{LL} \sim (A/K)^{1/2} \sim 10\text{–}0.1\,\mu\text{m}, \tag{3}$$

where *A* is the exchange constant and *K* is the anisotropy energy of the microwire ($K \sim \lambda\sigma$, where λ is the magnetostriction constant and σ is the effective residual stress from the fabrication procedure (see [2, 3] and Eq. (1)). The full theory gives $\Delta_f \sim 0.1$ μm for the size of the domain wall of glass-coated microwires (see [5]).

3. The radius of a single domain (according to Brown theory) is

$$a \sim A^{1/2} / M_S \sim 0.1\text{–}0.01 \mu\text{m}, \tag{4}$$

Where M_s is the saturation magnetization of microwire.

According to [2, 3], the frequency of the NFMR is

$$\left(\frac{\omega}{\gamma}\right)^2 = (H_e + 2\pi M_S)^2 - (2\pi M_S)^2 \exp(-2\delta / r), \tag{5}$$

Where γ is the gyromagnetic ratio ($\gamma \sim 3$ MHz/Oe). The anisotropy field is $H_e \sim 3\lambda\sigma/M_s$ (for exact calculations of anisotropy field, see below).

If $r<\delta$, we have

$$\frac{\omega}{\gamma} = H_e + 2\pi M_S. \tag{6}$$

If $r>\delta$, the NFMR frequency is given by (see [1−3])

$$\left(\frac{\omega}{\gamma}\right)^2 = H_e (H_e + +4\pi M_S). \tag{7}$$

The discovery of NFMR in amorphous microwires [3] was preceded by the study of the wires using standard FMR methods [4]. Then, a shift in the resonant field due to core deformation of the microwire associated with fusing of the glass and the core at the temperature of microwire formation was observed. The FMR line width is also of interest because it characterizes, in particular, the structural parameters [2, 3].

Since the skin penetration depth of a microwave field in a metallic wire is relatively small in comparison with its diameter, the resonant frequency of FMR can be determined by means of Kittel formula (Eqs. (6)−(8)). Taking into account the magnetoelastic stress field [2, 3], for a thin film magnetized parallel to the surface, we can obtain

$$\left(\frac{\omega}{\gamma}\right)^2 = (H + (N'_Z - N'_X) M_S + 4\pi M_S) \times (H + (N'_Z - N'_Y) M_S), \tag{8}$$

Where H is the FMR field; N'_X, N'_Y, N'_Z are the components of tensor of effective demagnetizing factors in the case of magnetoelastic stress:

$$N'_i = \frac{3|\lambda|\sigma i}{2M_S^2}\left(\cos^2 \theta i - \frac{1}{3}\right); \tag{9}$$

where

$\theta_1 = \theta_2 = 90^\circ, \theta_3 = 0.$

Components σ_i (see Eqs. (1)) are residual stresses (see [2, 3]). Then,

$$N'_X = N'_Y = -\frac{|\lambda| P}{2M_S^2};$$
$$N'_Z = \frac{|\lambda| P}{2M_S^2}\frac{(k+1)x+2}{kx+1}; \tag{10}$$

Substituting the σ_i values obtained in our previous work [2,3] (see Eqs. (1)), and taking into account Eqs. (8) and (9), we can calculate conditions for FMR:

$$\left(\frac{\omega}{\gamma}\right)^2 = \left[H + \frac{(3|\lambda| P)}{2M_S}\frac{x\left(k+\frac{2}{3}\right)+\frac{5}{3}}{kx+1} + 4\pi M_S\right]$$
$$\times\left[H + \frac{(3|\lambda| P)}{2M_S}\frac{x\left(k+\frac{2}{3}\right)+\frac{5}{3}}{kx+1}\right] . \tag{11}$$

.

If the glass is removed, the stress is completely removed. Then the FMR resonant field of wire without glass casing H_0 is determined from

$$\left(\frac{\omega}{\gamma}\right)^2 = H_0(H_0 + +4\pi M_S) \tag{12}$$

We have shown (see [1−4, 6−8]) that these relations quantitatively explain all of the basic features of NFMR and FMR. Note that the value of M_S required for the calculations was determined both by standard methods on a vibration magnetometer and with the use of interpolation formulas given here. The error relative to tabular values for the given alloys is not greater than 5%.

For the frequency of NFMR under the simple approximation taking εE_1~ 2GPa and k~ 0.4, this formula can be written as

$$\omega(GHz) \approx \omega o\left(\frac{0.4x}{0.4x+1}\right)^{1/2}$$
$$\omega o(GHz) \approx 1{,}5(10^6\lambda)^{1/2} \tag{13}$$

It is evident that the dependence for the frequency of NFMR (Eqs. (13), and Figs. 2, 3) is determined from two typical values x, λ.

The basic contribution to the NFMR frequency and NFMR line width is due to the effective magnetostriction and parameter x (Eqs. (13), and Figs. 2, 3, 5). The residual stress in the microwire plays the dominant role in the formation of the absorption line width, as will be shown below (Figs. 5, 6).

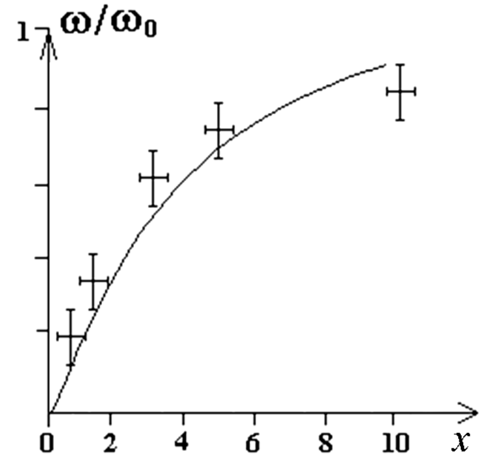

Fig. 2. Theoretical curve of NFMR frequency as a function of *x* (according to Egs. (11)–(13)) and experimental data (see [2, 3]).

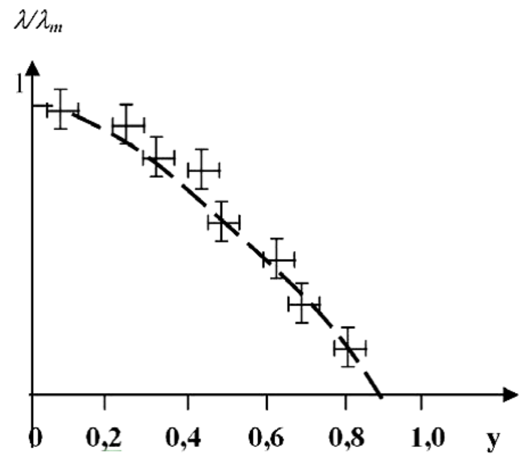

Fig. 3. Dependence of relative magnetostriction λ/λ_m for alloy composition $(Co_y\ Fe_{1-y})_{75}(BSiC)_{25}$ series cast glass-coated amorphous magnetic microwires according to Eqs. (11)–(13), where y = Co/(Co+Fe) (see [2, 3]).

When the penetration depth of the microwave field in the metallic wire is small relative to the wire diameter (on account of the skin effect), the resonant frequency in FMR and NFMR can be determined by means of Eqs. (1). (The general theory of residual tension is presented in [5]; however, here it is enough to use the simple theory from [2, 3]).

Substituting typical values of λ and x in Eq. (13), we reach numerical values of NFMR in a range of 1−12 GHz. A systematic study on the NFMR frequency for the alloy series $(Co_yFe_{100-y})_{75}(BSiC)_{25}$ has been performed as a function of the Co content (Fig.3). The magnetostriction has then been evaluated using Eq. (13). The result is plotted in Fig. 3 which shows good agreement with the magnetostriction values as determined through conventional techniques (Fig.4. according to [9]). Thus, the final theory quantitatively explains all the basic features of NFMR and FMR. However, the area of experimental research in the case of a small radius of the metallic nucleus of a microwire remains vacant.

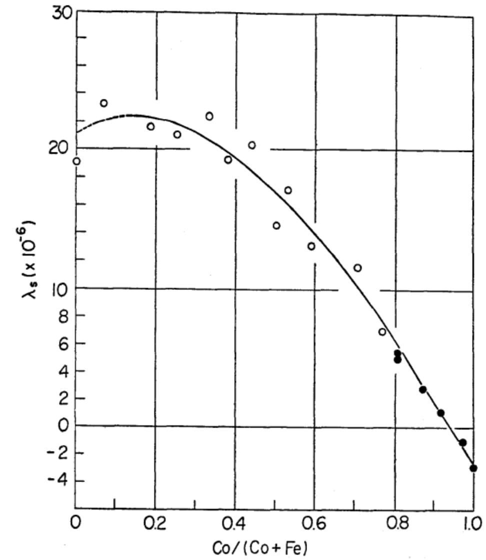

Fig. 4. Typical saturation magnetostriction λ_s in the amorphous Co–Fe alloys: ○ $(Fe_{1-y}Co_y)_{80}(PC)_{20}$; ● $(Fe_{1-y}Co_y)_{75}(SiB)_{25}$ (according to [9]).

3. Radio-absorption shielding

NFMR occurs when the sample is submitted to a microwave field without application of any biasing field other than the intrinsic anisotropy field of the microwire.

Near the NFMR frequency, the dispersion of permeability μ given by

$$\mu(\omega) = \mu'(\omega) + i\,\mu''(\omega), \tag{14}$$

exhibits a peak in μ'' and a zero crossing of μ' .

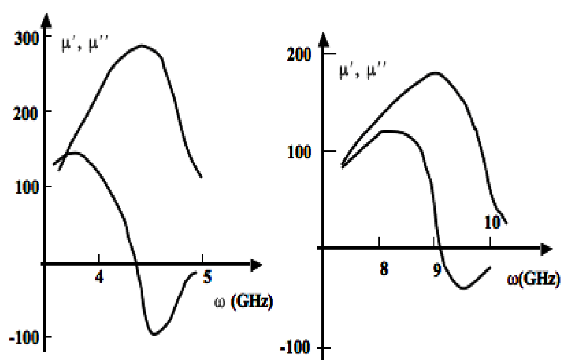

(a) (b)

Fig. 5. Real and imaginary relative permeability components around NFMR for $Co_{59}Fe_{15}B_{16}Si_{10}$ (a) and $Fe_{69}C_5B_{16}Si_{10}$ (b) microwires (*r*~ 5 μm, *x* > 8 (see [10])).

Figures 5a and 5b show resonance frequencies of 4.4 and 9.0 GHz and resonance widths of 1 and 0.5 GHz for two compositions. Near resonance μ" is expected to be described by

$$\mu''/\mu_{dc} \sim \Gamma\Omega / [(\Omega - \omega)^2 + \Gamma^2], \tag{15}$$

where μ_{dc} is static magnetic permeability and Γ is the width of the resonant curve. Very near resonance, when $\Gamma > (\Omega - \omega)$, Eq. (15) reduces to

$$\mu''/\mu_{dc} \sim \Omega / \Gamma \sim 10\text{–}10^2.$$

Note that, in Fig. 5a, the imaginary component is rather symmetrically distributed around the resonance frequency. This is due to the symmetric distribution of the circular permeability in the near surface layer within the penetration depth. In contrast, in Fig. 5b, the imaginary component shows a non-symmetric feature around the resonance frequency. This can be attributed to the inhomogeneous pattern of permeability in the region close to the surface of the microwire where metastable phases occur, as demonstrated by X-ray studies.

Monitoring the geometry of the microwire (i.e., its diameter) and the magnetostriction through its composition makes it possible to prepare microwires with tailorable permeability dispersion for designing radio-absorption materials:
(i) Determining the resonant frequency in a range of 1−12 GHz;
(ii) Controlling the maximum of the imaginary part of magnetic permeability.

High-frequency properties, pieces of microwires have been embedded in planar polymeric matrices to form composite shielding for radio absorption protection. Experiments have been performed employing commercial polymeric rubber with a thickness of about 2−3 mm. Microwires are spatially randomly distributed within the matrix before its solidification. Concentration is maintained below 8−10g of microwire dipoles (1−3mm long) per 100g of rubber [11]. A typical result obtained in an anechoic chamber is shown in Fig. 6 for a screen with embedded $Fe_{69}C_5B_{16}Si_{10}$ microwires. As observed, an absorption level of at least 10 dB is obtained in a frequency range of 8−12 GHz with a maximum attenuation peak of 30 dB at around 10 GHz. In general, optimal absorption is obtained with microwires with metallic nuclei of diameter $2r$ = 1−3 μm (2R ~ 20μm (x > 10)) and length L = 1−3 mm. These pieces of microwires can be treated as dipoles whose length L is comparable to the half value of the effective wavelengths $\Lambda_{eff}/2$ of the absorbed field in the composite material (i.e., in connection to a geometric resonance).

Figure 6 also shows how the frequency absorption spectrum of shielding with $Fe_{69}C_5B_{16}Si_{10}$ microwires changes when it is rotated (90º each spectrum).

We attribute the changing attenuation to the lack of perfect angular distribution of microwires whose length does not always fit within the shielding thickness.

The effect does not even have mirror symmetry. (The measurement error was less than 10% for the frequency, and while the spread of the attenuation factor was 5 dB).

Small fluctuations in concentration of dipoles at a concentration of dipoles near the percolation threshold can lead to fluctuation of the absorption curve. Similar results were presented in [12].

As observed, both frequency dependences (Figs. 5b and 6) are similar except for the half-width value of the permeability.

Although the design of absorption shielding can be based on disposing the dipolar pieces in a stochastic way, we consider, for simplicity, a theoretical analysis for a diffraction grating with spacing between wires Q < Λ (Λ is wavelength of absorbed field). (Another simple example is in Appendix A).

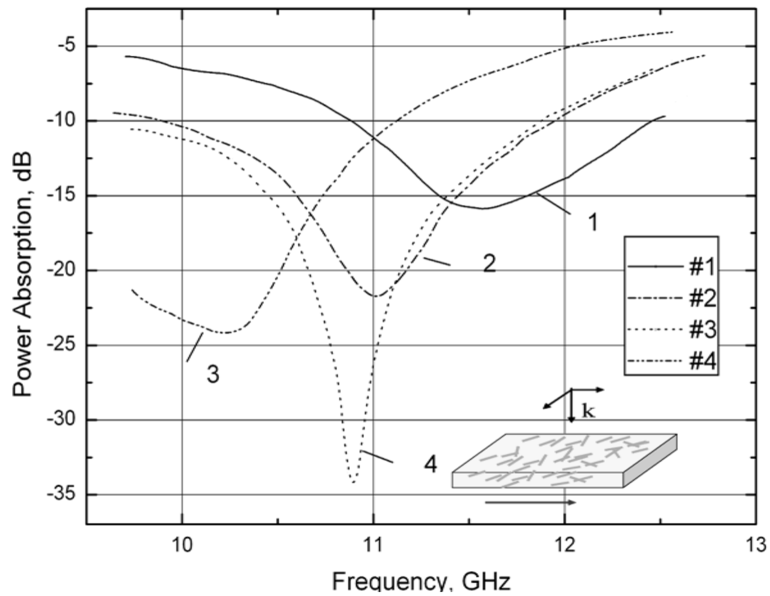

Fig. 6. Absorption characteristics of shielding by a microwire composite with NFMR in the HF-field in a frequency range of 10−12 GHz. Curve 1 represents an initial situation of the screen; (2−4): the screen is turned by 90° about a perpendicular axis each time.

The propagation of an electromagnetic wave through absorption shielding with microwire-based elements is characterized by transmittance $|T|$ and reflectance $|R_r|$ coefficients given by

$$|T| = (\alpha^2 + \beta^2)/[(1+\alpha)^2 + \beta^2];$$

$$|R_r| = 1/[(1+\alpha)^2 + \beta^2], \tag{16}$$

where $\alpha = 2X_r/Z_0$, and $\beta = 2\,Y/Z_0$, with $Z_0 = 120\pi/Q$, and the complex impedance $Z = X_r + iY$.

Absorption function $G$is correlated with the generalized high-frequency complex conductivity Σ (or high-frequency impedance Z).

Here, we use the analogy between the case of a conductor in a waveguide and that of a diffraction grating. The absorption function, given by

$$|G| = 1 - |T|^2 - |R_r|^2 = 2\alpha / [(1+\alpha)^2 + \beta^2] \quad , \tag{17}$$

has a maximum

$$|G_m| = 0.5 \geq |G|,$$

for simultaneous $\alpha=1$ and $\beta=0$, for which
$|T|^2 = |R_r|^2 = 0.25$.

The minimum $|G|=0$ occurs at $\alpha=0$, β of any positive number).

Theoretical estimations taking into account only the active resistance of microwires result in attenuation within a range of 5−15 dB being much lower than experimental results, which for spacing of microwires Q $=10^{-2}$ m ranges between 18 and 15 dB, while for a spacing Q $= 10^{-3}$ m it increases up to 20−40 dB. Thus, it becomes clear that shielding exhibits anomalously high absorption factors, which cannot be explained solely by the resistive properties of microwires.

The high-frequency conductivity Σ_m of a stochastic mixture of microwires in the polymeric matrix can be expressed as a function of conductivities Σ_i of non-conducting (polymeric matrix) and conducting (microwire) elements, denoted by subscripts 1 and 2, respectively, as follows [13]:

$$\Sigma_m = B + (B^2 + A\,\Sigma_1\,\Sigma_2)^{1/2}, \qquad (18)$$

where

$$B=1/2\{[\Sigma_1(X_1-AX_2)+\Sigma_2(X_2-AX_1)]\};$$

X_i is the fractional volume:

$$(X_1+X_2)=1;$$

$$A=1/(J_1-1), \text{ with } \qquad J_1\sim (J+Y/X_r)$$

being the fractal dimension of the system (J is the geometrical dimension of the system) and

$$Y/X_r \sim (r/\delta)^2.$$

Figure 7 shows that, in case of a thick microwire ($r > \delta \approx 1\,\mu$m), the conductivity of the system becomes very high, even in case of a low microwire concentration, indicating the case of an antenna resonance as reported in [11].

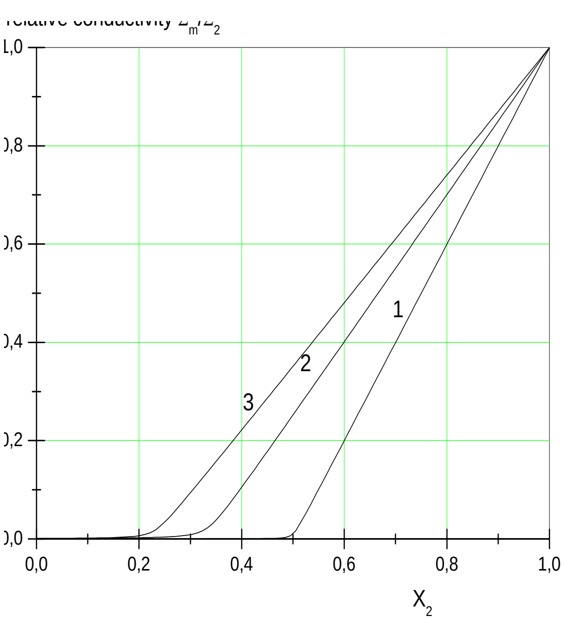

Fig. 7. Generalized conductivity calculated using Eq. (18) for $\Sigma_2 / \Sigma_1 \sim 10^4$: (*1*) thin microwire ($r< \delta \sim 1$ μm) J = 2, Y = 0; (*2*) thin microwire ($r < \delta \sim 1$ μm) J = 3, Y = 0; and (*3*) thick microwire ($r > \delta \sim 1$ μm) $J_1 = 4$, $Y/X_r = 1$.

Let us consider the effective absorption function (as in Eq. (17)):

$$|G_{eff}| \sim \Gamma_{eff}\,\Omega_{eff}/\,[(\Omega_{eff} - \Omega)^2 + \Gamma_{eff}^2], \tag{19}$$

where $\Gamma_{eff} \geq \Gamma$ (see Eq. (12)) and $\Omega \sim \Omega_{eff}=2\pi c/\Lambda$.
A microwave antenna will resonate when its length, L, satisfies

$$L \sim \Lambda/\,2(\mu_{eff})^{1/2}. \tag{20}$$

The maximum absorption (see Fig. 6) occurs for $\Omega_{eff} \sim 10$ GHz ($\Lambda \sim 3$ cm) and $\mu_{eff} \sim 10^2$, (according to Fig. 5). This corresponds to

$$L \sim 1.5\text{–}2 \text{ mm}, \tag{21}$$

where the microwire concentration (see Fig.7) $X_2<0.2$) is much less than the percolation threshold. A greater concentration of dipoles increases absorption, $|G_{eff}|$, but also increases reflectance, $|R_{r1}|$, which can be simply evaluated to be [14]:

$$|R_{r1}| \sim 1 - 2\sqrt{(\Omega/2\pi\Sigma_m)}, \tag{22}$$

Where $\Omega/2\pi \sim 10^{10}$ Hz.

The formula is applicable, and calculation of small reflectance, $|R_{r1}|$ is possible, only if

$$\Sigma_m \sim 10^{11}\text{Hz},$$

for concentration below the percolation threshold (as $\Sigma_2 \sim 10^{15}$Hz).

Thus, for very thin microwires (i.e., thinner than 1 μm in diameter) embedded in a composite matrix with concentration larger than the percolation level $X_2 \sim 0.2$, a noticeable absorption effect should be expected.

4. Conclusions

The microwave electromagnetic response has been analyzed for a composite consisting of dipoles of amorphous magnetic glass-coated microwires in a dielectric. This material can be employed for radio absorbing screening. The spontaneous NFMR phenomena observed in glass-coated microwires has opened the possibility of developing novel materials with broad-band of radio absorbing materials.

Acknowledgments. This research received financial support from the Department of Engineering Physics *École Polytechnique de Montréal.* The author thanks A. Yelon and D. Menard for their participation in discussions of the results.

Appendix A

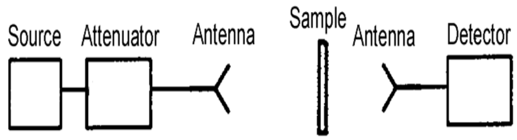

It is well known, that the simple model of contact of vacuum with the absorbing material gives the following equations [14] (the general theory is presented in [15]; see also [16]):

$$1+ R_r = T, \tag{A. 1}$$

$$(\alpha+i\,\beta)(1- R_r)= T;$$

that gives

$$R_r = \frac{1-\alpha-i\beta}{1+\alpha+i\beta}, \tag{A. 2}$$

and at β =0 , α =1 ,we find

$$R_r =0. \tag{A. 3}$$

From these findings, it is possible to obtain a simple criterion for matching the vacuum with a radio absorbing material:

$$\mu_m \sim \Sigma_m / \Omega, \tag{A. 4}$$

(where μ_m is the effective magnetic permeability of the composite). This condition cannot be satisfied for composites containing amorphous magnetic wires. This fact forces us to use other physical principles for designing radio absorbing materials presented above).

We note that similar results were obtained in [16].

References

[1] A.N. Antonenko, S.A. Baranov, V.S. Larin, and A.V. Torcunov, Suppl. Mater. Sci. Eng. A 248, (1997).
[2] S.A. Baranov, V.N. Berzhansky, S.K. Zotov,V.L. Kokoz, V.S. Larin, and A.V. Torcunov, Fiz. Met. Metalloved. 67 , 73, (1989).
[3] S.A. Baranov, S.K. Zotov, V.S. Larin, andA.V. Torcunov, Fiz. Met. Metalloved. 69, 172, (1991).
[4] L. Kraus, Z. Frait, and I. Schneider, Phys. Stat. Sol. A 63, 669, (1981).
[5] S.A. Baranov,Surf. Eng. Appl. Electrochem. 47, 316, (2011).
[6] F. Yıldız, B.Z. Rameev, S.I. Tarapov,L.R. Tagirov, and B. Aktas,J. Magn. Mag. Mater. 247, 222, (2002).

[7] M. Vazquez and A.-L. Adenot-Engelvin, J. Magn. Mag. Mater. 321, 2066, (2009)
[8] D. Menard and A. Yelon, J. Appl. Phys. 88, 379, (2000).
[9] H. Fujimori, M. Kikuchi, Y. Obi, andT. Masumoto. New Co-Fe Amorphous Alloys as Soft Magnetic Materials. The 1659th report of Research Institute for Iron, Steel and Other Metals, 46 p., 1976.
[10] S. A. Baranov, J. Commun. Tech. Electron. 48, 226, (2003).
[11] S. A. Baranov, Tech. Phys. Let. 24, 549, (1998).
[12] A. P. Vinogradov, D. P. Makhnovskii, and K. N. Rozanov, J. Commun. Tech. Electron. 44, 317, (1999).
[13] S. A. Baranov, Tech. Phys. 44, 853, (1999).
[14] M. Born and E. Wolf, Principles of Optics: Electromagnetic Theory of Propagation, Interference and Diffraction of Light, Oxford–New York:Pergamon press, 1969.
[15] H.W. Bode, Network and Feedback Amplifier Design, Princeton: van Nostrand, 1945.
[16] Mingzhong Wu, Huahui He, Zhensheng Zhao, and Xi Yao,J. Phys. D: Appl. Phys. 33, 2398, (2000).